# Isentropic Compressibility, Electrical Conductivity, Shear Relaxation Time, Surface Tension, and Raman Spectra of Aqueous Zinc Nitrate Solutions

**Abdul Wahab and Sekh Mahiuddin***

Material Science Division, Regional Research Laboratory, Jorhat 785 006, Assam, India

The speed of sound, electrical conductivity, viscosity, surface tension, and Raman spectra of aqueous zinc nitrate solutions were measured from dilute to very high concentrations as a function of temperature ($273.15 \leq T/K \leq 323.15$). Isentropic compressibility isotherms converge at 2.18 mol·kg$^{-1}$ and provide crucial structural information regarding ion hydration. At the converging concentration, 26.3 water molecules are rigidly bound in the primary hydration shell of $Zn^{2+}$ and $NO_3^-$ ions. The hydrated $Zn^{2+}$ and $NO_3^-$ ions up to 2.2 mol·kg$^{-1}$ and beyond 2.2 mol·kg$^{-1}$, solvent-separated and/or solvent-shared ion pairs govern the transport properties.

## Introduction

In continuation of a series of studies,[1−4] transport and acoustic properties and spectroscopic investigations have been performed over a wide range of concentrations and temperatures to provide physical insight concerning the ionic species present in electrolyte solutions. For instance, the saturation of the primary hydration shell of ions and elucidation of the structure of hydrated ions could be characterized by the variation of isentropic compressibility isotherms with concentration in conjunction with the electrical conductivity, shear relaxation time, and vibration spectra.[3]

Zinc nitrate, being highly soluble in water and a promising salt for high energy density batteries, deserves a comprehensive investigation. Vibration spectral studies of aqueous zinc nitrate solution in a wide range of concentrations have been reported.[5] However, a systematic investigation of acoustic and transport properties as functions of concentration and temperature for the system is lacking in the literature. Most of the data available in the literature[6,7] concern only at 298.15 K. Carpio et al.[8] reported the speed of sound at 323.15 K for aqueous zinc nitrate, calcium nitrate, and zinc chloride solutions. They interpreted the extent of metal aqua complexation behavior from isentropic and excess isentropic compressibility.

Vibrational spectra are sensitive to the stretching frequencies of free or bound ions. Raman bands at (≈390, 719, 740, 1048, and 1400) cm$^{-1}$ are sensitive to the water molecules around the $Zn^{2+}$ and $NO_3^-$ ions, and the existence of different ionic species or complexation is characterized by the appearance of new bands or by splitting of bands. The ionic interactions (ion−solvent and ion−ion) and the constituent hydrogen-bonding aspect in hydrogen-bonded solvents in different concentration regions primarily govern the physicochemical properties of the electrolyte solutions. In this paper, the speed of sound, electrical conductivity, viscosity, surface tension, and Raman spectra of aqueous zinc nitrate solutions are reported in order to sort out different kinds of interaction and ionic species present in different concentration ranges.

* Corresponding author. Fax no. 0091-376-2370011. E-mail: mahirrljt@yahoo.com.

## Experimental Section

Analytical grade $Zn(NO_3)_2 \cdot 6H_2O$ (>98%, CDH, India) was recrystallized twice from double-distilled water and then kept in a vacuum desiccator over $P_2O_5$. A stock solution was prepared by volume with double-distilled water. Solutions of interest were prepared by successive dilution of stock solution with an uncertainty of ±0.2%, and the concentration was finally checked by EDTA titration.

Measurements of speed of sound, $u$, at 2 MHz, density, $\rho$, and viscosity, $\eta$, and recording of Raman spectra were carried out as described elsewhere.[2,3] Uncertainties in the speed of sound, density, and viscosity measurements were within ±0.01%, ±0.01%, and ±0.5%, respectively. The wavenumber accuracy in the Raman spectral measurement was ±1 cm$^{-1}$. All spectral measurements were made at least three times to ensure reproducibility. The Raman spectra were recorded at room temperature.

Electrical conductivity, $\kappa$, was measured using a platinized platinum cell having a cell constant = 1.09 cm$^{-1}$ and an autoranging conductivity meter (TCM15, Toshniwal, India) at 3 kHz. The cell constant was determined by using a 0.1 mol·kg$^{-1}$ aqueous KCl solution at different temperatures, and the conductivity of some standard electrolyte solutions was also checked to ascertain the cell constant. The overall uncertainty in the conductivity measurements was within ±0.5%.

Surface tension, $\sigma$, of all the solutions was measured with an automatic tensiometer (dynamic contact angle meter and tensiometer, DCAT-11, Dataphysics, Germany) using the Wilhelmy plate method with an accuracy of ±0.01 mN·m$^{-1}$. Triplicate measurements were made at each temperature and concentration.

All measurements were performed as functions of concentration ($0.0875 \leq m/(\text{mol·kg}^{-1}) \leq 7.764$) and temperature ($273.15 \leq T/K \leq 323.15$) except Raman spectra. A thermostat type Schott-Geräte CT 1450 or Julabo F32 HP was used to control the temperature of the solutions within ±0.02 K.

## Results and Discussion

Measured densities are listed in Table S1 (Supporting Information). Experimental density data agree well within

10.1021/je0302001 CCC: $27.50 
Published on Web 11/15/2003

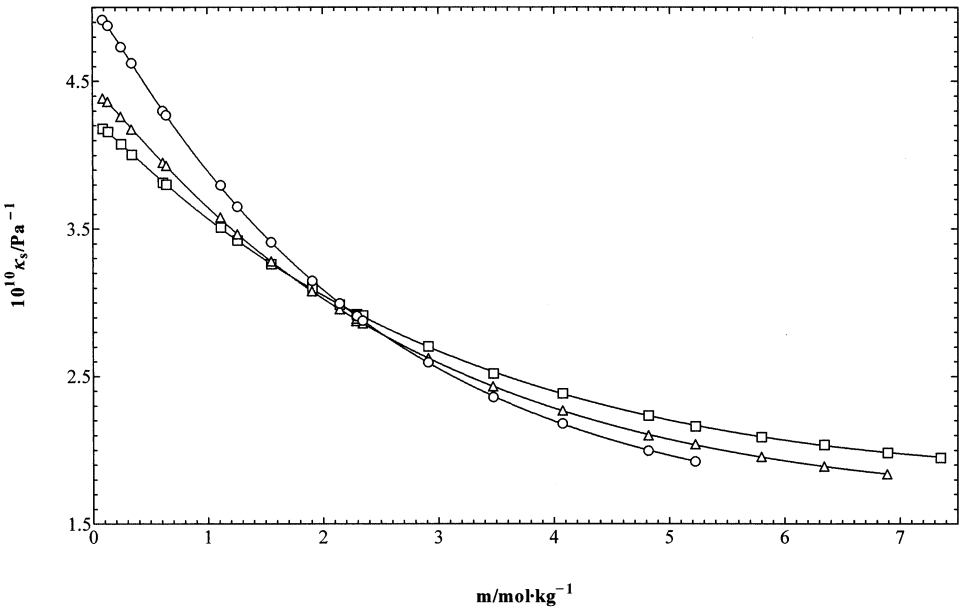


**Figure 1.** Variation of isentropic compressibility, $\kappa_s$, with molality, $m$, at (○) 273.15 K, (△) 298.15 K, and (□) 323.15 K for aqueous zinc nitrate solutions (symbols and solid curves represent experimental and fitted (from eq 2) values, respectively).

**Table 1. Least-Squares Fitted Values of the Parameters of Eq 2 for Aqueous Zinc Nitrate Solutions**

| parameter | 273.15 K | 278.15 K | 283.15 K | 288.15 K | 293.15 K | 298.15 K | 308.15 K | 313.15 K | 318.15 K | 323.15 K |
|---|---|---|---|---|---|---|---|---|---|---|
| $10^{10}A$/Pa$^{-1}$ | 4.871 | 4.716 | 4.598 | 4.495 | 4.396 | 4.349 | 4.201 | 4.195 | 4.193 | 4.159 |
| | ±0.024 | ±0.016 | ±0.020 | ±0.018 | ±0.016 | ±0.025 | ±0.058 | ±0.015 | ±0.059 | ±0.023 |
| $10^{10}B$/(mol$^{-1/2}$·kg$^{1/2}$·Pa$^{-1}$) | 0.9438 | 0.9208 | 0.8345 | 0.8013 | 0.8182 | 0.6803 | 0.7799 | 0.6114 | 0.4539 | 0.5020 |
| | ±0.0994 | ±0.0656 | ±0.0779 | ±0.0700 | ±0.0575 | ±0.0920 | ±0.2105 | ±0.0534 | ±0.2139 | ±0.0832 |
| $10^{10}C$/(mol$^{-1}$·kg·Pa$^{-1}$) | −3.028 | −2.839 | −2.573 | −2.427 | −2.353 | −2.105 | −2.104 | −1.822 | −1.552 | −1.615 |
| | ±0.131 | ±0.087 | ±0.098 | ±0.085 | ±0.067 | ±0.108 | ±0.241 | ±0.061 | ±0.245 | ±0.096 |
| $10^{10}D$/(mol$^{-3/2}$·kg$^{3/2}$·Pa$^{-1}$) | 1.270 | 1.177 | 1.038 | 0.9696 | 0.9347 | 0.8167 | 0.8243 | 0.6782 | 0.5376 | 0.5891 |
| | ±0.070 | ±0.046 | ±0.049 | ±0.0409 | ±0.0312 | ±0.0501 | ±0.1091 | ±0.0278 | ±0.1115 | ±0.0435 |
| $10^{10}E$/(mol$^{-2}$·kg$^{2}$·Pa$^{-1}$) | −0.1628 | −0.1500 | −0.1278 | −0.1185 | −0.1144 | −0.0961 | −0.1003 | −0.0757 | −0.0519 | −0.0636 |
| | ±0.0129 | ±0.0086 | ±0.0087 | ±0.0069 | ±0.0050 | ±0.0081 | ±0.0171 | ±0.0044 | ±0.0175 | ±0.0068 |
| std dev in $\kappa_s$ | 0.004 | 0.003 | 0.004 | 0.004 | 0.004 | 0.005 | 0.011 | 0.004 | 0.011 | 0.006 |

±0.2% with the reported data.[6,7] The speeds of sound in aqueous zinc nitrate solutions are presented in Table S2 (Supporting Information) as functions of concentration and temperature. Experimental speed of sound values are comparable within ±0.4% with the data of Carpio et al.[8] The electrical conductivities of aqueous zinc nitrate solutions are recorded in Table S3 (Supporting Information) as functions of concentration and temperature. The deviation between the measured and the reported conductivity values[9] is estimated to be within ±2% at 291.15 K. The measured viscosities of aqueous zinc nitrate solutions at various concentrations and temperatures are presented in Table S4 (Supporting Information). The viscosity values are in agreement within ±3.5% with the literature data at 298.15 K.[7] The surface tensions of aqueous zinc nitrate solutions measured at different temperatures are listed in Table S5 (Supporting Information) as a function of concentration. The measured $\sigma$ values agree within ±0.8% with the literature data at 313.15 K.[10]

***Isentropic Compressibility.*** Isentropic compressibility, $\kappa_s$, was calculated using the Newton−Laplace equation:

$$\kappa_s = (u^2\rho)^{-1} \tag{1}$$

The isentropic compressibilities are plotted against concentration at three temperatures and depicted in Figure 1. An isothermal equation[11] of the following form was used

$$\kappa_s = A + Bm^{1/2} + Cm + Dm^{3/2} + Em^2 \tag{2}$$

to fit the isentropic compressibilities, and the least-squares fitted values of the parameters of eq 2 are summarized in Table 1. In eq 2, $A$, $B$, $C$, $D$, and $E$ are temperature-dependent parameters and $m$ is the concentration in mol·kg$^{-1}$.

It is apparent from Figure 1 that the isentropic compressibility isotherms converge at a particular concentration range, which is characteristic of aqueous electrolyte solutions. The variation of $\kappa_s$ versus $m$ plots (Figure 1) reveals the fact that as the electrolyte is added, the isentropic compressibility of the solution at a particular temperature is decreased due to the combined effect of hydration of ions and breaking of the three-dimensional network structure of water. From the variation of the compressibility isotherms (Figure 1) it is assumed that in aqueous electrolyte solutions the isentropic compressibility is the sum of two contributions: $\kappa_{s(\text{solvent intrinsic})}$ and $\kappa_{s(\text{solute intrinsic})}$. Therefore, following the explanation for a water−ammonia mixture by Bowen et al.,[12] we may write

$$\kappa_s = \kappa_{s(\text{solvent intrinsic})} + \kappa_{s(\text{solute intrinsic})} \tag{3}$$

where $\kappa_{s(\text{solvent intrinsic})}$ is the isentropic compressibility due to the compression of the three-dimensional network structure of water and $\kappa_{s(\text{solute intrinsic})}$ is the isentropic compressibility due to the compression of the hydration shell of ions and interionic distance. $\kappa_{s(\text{solvent intrinsic})}$ is the dominant contributor to the total value of $\kappa_s$ from pure solvent up to the converging concentration, and beyond that $\kappa_{s(\text{solute intrinsic})}$ is the substantial contributor.

**Table 2. Reported Primary Hydration Number of Zinc and Nitrate Ions Determined Using X-ray (X) and Neutron (N) Diffraction, Extended X-ray Absorption Fine Structure (EXAFS), Raman Spectra (R), Molecular Dynamics (MD), Monte Carlo (MC), ab Initio, and Density Functional Theory (DFT) Simulation Techniques**

| ion | concentration | hydration number | technique | refs |
|---|---|---|---|---|
| $Zn^{2+}$ | | 5.9−6.6 | X | 13 (Table 2) |
| | 2.37 mol·kg$^{-1}$ | 5.9 | X | 14 |
| | 1.0 mol·dm$^{-3}$ | 6.2 | X | 15 |
| | 4.72 mol·dm$^{-3}$ | 6.6 | X | 16 |
| | 2.0 mol·kg$^{-1}$ | 5.3 | N | 17 |
| | (2.7−0.005) mol·kg$^{-1}$ | 6 | EXAFS | 18 |
| | | 6 | EXAFS | 19 |
| | (1.3−3.5) mol·dm$^{-3}$ 3.36 mol·kg$^{-1}$ | 6 | R | 5, 20, 21 |
| | | 6 | EXAFS & MD | 22 |
| | 0.28 mol·kg$^{-1}$ | 4−7 | MC | 23 |
| | | 6 | MC | 24 |
| | | 6 | ab initio | 25, 26 |
| | | 5, 6 | ab initio | 27 |
| | | 4, 6 | DFT | 28 |
| | | 4, 5, 6 | DFT | 29 |
| | | 6 | DFT | 30, 31 |
| $NO_3^-$ | 4.72 mol·dm$^{-3}$ | 9 | X | 16 |
| | | 1.3−17.7 | X & N | 13 (Table 7) |

To quantify the concentration at which $\kappa_s$ isotherms converge, the temperature derivative of $\kappa_s$ appears to be important. At the converging concentration (2.18 mol·kg$^{-1}$, Figure 1), $d\kappa_s/dT = 0$, which implies that $d\kappa_{s(\text{solvent intrinsic})}/dT = 0$ and $d\kappa_{s(\text{solute intrinsic})}/dT = 0$. It seems that, at 2.18 mol·kg$^{-1}$, the intrinsic water structure is completely broken and all the water molecules are incorporated in the primary hydration shell of the ions. Below 2.18 mol·kg$^{-1}$, $d\kappa_s/dT < 0$, so that $d\kappa_{s(\text{solvent intrinsic})}/dT < 0$, and above 2.18 mol·kg$^{-1}$, $d\kappa_{s(\text{solute intrinsic})}/dT > 0$ where the contribution from $\kappa_{s(\text{solvent intrinsic})}$ is virtually nil.

The hydration number, $n_h$, was calculated using the reported empirical equation[2]

$$n_h = (\kappa_{s,\phi} - \kappa_{s,h}V_\phi)/[V_1(\kappa_{s,h} - \kappa_{s,1})] \quad (4)$$

where $\kappa_{s,\phi}$ is the conventional apparent molal isentropic compressibility of the solute, $V_\phi$ is the apparent molal volume of the solute, $\kappa_{s,h}$ is the isentropic compressibility of the primary hydration shell, and $\kappa_{s,1}$ and $V_1$ are the isentropic compressibility and the molar volume of the solvent, respectively. The total primary hydration number for zinc and nitrate ions at 2.18 mol·kg$^{-1}$ was estimated from eq 4 and was found to be 26.3 and is in good agreement with the available number of water molecules per mole of the solute (25.5) at that concentration.

A number of studies have been reported to elucidate the structure of aqueous zinc nitrate solutions using different experimental[13−21] and theoretical[13,22−31] techniques. For easy comparison, the primary hydration numbers obtained from different techniques are summarized in Table 2. Most of the techniques reported hexacoordination to $Zn^{2+}$(aq). Bulmer et al.[20] showed that $Zn(H_2O)_6^{2+}$ is a stable complex from low-frequency Raman spectra. Recently, Muñoz-Páez et al.[19] studied aqueous zinc nitrate solutions in a wide concentration range from (0.005 to 2.7 mol·kg$^{-1}$) using extended X-ray absorption fine structure (EXAFS) and observed no change in the hexacoordinated primary hydration shell of $Zn^{2+}$ ion with concentration. Further, they reported a decreasing trend of hydration number in the secondary hydration shell with increasing concentration. Very recent studies[22] have concluded that six water molecules are tightly bound to $Zn^{2+}$ ion in the first hydration shell and beyond the first hydration shell the structural information gained from the EXAFS technique is not reliable.

Therefore, the total primary hydration number (26.3) of zinc nitrate was bifurcated into ionic contributions by assuming a stable and hexahydrated primary hydration shell of $Zn^{2+}$ ion. The remaining waters (20.3) are hydrogen-bonded to two $NO_3^-$ ions by at least each nitrate O-atom bonded to three water molecules, resembling the conclusion drawn by Dagnall et al.[16] The positively charged nitrogen atom of the $NO_3^-$ may also interact with another one or two water molecules.[13]

***Electrical Conductivity.*** The conductivity data were analyzed by applying the Casteel−Amis equation[32]

$$\kappa = \kappa_{max}(m/\mu)^{a_2} \exp[b_2(m - \mu)^2 - a_2(m - \mu)/\mu] \quad (5)$$

where $\mu$ is the concentration corresponding to the maximum conductivity, $\kappa_{max}$, at a given temperature and $a_2$ and $b_2$ are the empirical parameters. Least-squares fitted values of the parameters of eq 5 are summarized in Table 3.

The $\kappa$ versus $m$ isotherms at four temperatures along with the literature data are depicted in Figure 2. The variation of conductivity with concentration reflects a structural transition at (2.22 ± 0.09) mol·kg$^{-1}$. As the salt content increases, the size of the migrating entity decreases due to the departure of water molecules from the secondary hydration sphere giving more freedom to move. The departure of water molecules from the secondary hydration sphere is completed by the time $\kappa_{max}$ is reached (Table 3 and Figure 2) at (2.22 ± 0.09) mol·kg$^{-1}$. Whereupon, at >(2.22 ± 0.09) mol·kg$^{-1}$, available water molecules are shared by both $Zn^{2+}$ and $NO_3^-$ ions, resulting in solvent-separated and/or solvent-shared ion pairs of reduced charge and mobility. Thus, the conductivity pattern below (2.22 ± 0.09) mol·kg$^{-1}$ revealed the well-structured feature of ion hydration controlled by ion−water interactions, and beyond (2.22 ± 0.09) mol·kg$^{-1}$ the perturbed features of ion hydration controlled by ion−ion interactions are revealed. Consequently, coupling of these two controlling effects produces a maximum in the conductivity isotherm. It is interesting to note that the concentration at which $\kappa_{max}$ occurs reasonably coincides with the concentration at which isentropic compressibility isotherms converge (Figure 1).

***Shear Relaxation Time.*** To demarcate the concentration regions dominated by ionic species or specific complexes, shear relaxation time, $\tau$, was calculated using the equation

$$\tau = 4\kappa_s\eta/3 \quad (6)$$

The dependence of $\kappa$ on $\tau$ is illustrated in Figure 3 at 303.15 K and 323.15 K. From Figure 3, it is apparent that the conductivity increases sharply but the structural relaxation time remains fairly constant. The results imply that, up to 2.2 mol·kg$^{-1}$, the hydrated $Zn^{2+}$ and $NO_3^-$ ions exist and, beyond 2.2 mol·kg$^{-1}$, solvent-separated and/or solvent-shared $[Zn(H_2O)_6(NO_3)]^+$ ion pairs are largely formed.

***Surface Tension.*** The surface tensions were found to be a linear function of temperature at a fixed concentration having the following mathematical form:

$$\sigma = a_3 - b_3T \quad (7)$$

The least-squares fitted values of the parameters of eq 7 are summarized in Table 4. Surface entropy, $S_\sigma$, and

**Table 3. Least-Squares Fitted Values of the Parameters of Eq 5 for Aqueous Zinc Nitrate Solutions**

| $T$/K | $\kappa_{max}$/S·m$^{-1}$ | $\mu$/mol·kg$^{-1}$ | $a_2$ | $10^{-3}b_2$/kg$^2$·mol$^{-2}$ | std dev in $\kappa$ |
|---|---|---|---|---|---|
| 273.15 | 8.16 ± 0.02 | 2.241 ± 0.013 | 0.9044 ± 0.0169 | −0.0299 ± 0.0024 | 0.05 |
| 291.15 | 12.42 ± 0.05 | 2.314 ± 0.019 | 0.9110 ± 0.0304 | −0.0280 ± 0.0069 | 0.06 |
| 298.15 | 14.13 ± 0.05 | 2.222 ± 0.018 | 1.004 ± 0.019 | −0.0011 ± 0.0018 | 0.12 |
| 323.15 | 20.79 ± 0.07 | 2.312 ± 0.018 | 1.010 ± 0.017 | −0.0086 ± 0.0013 | 0.17 |

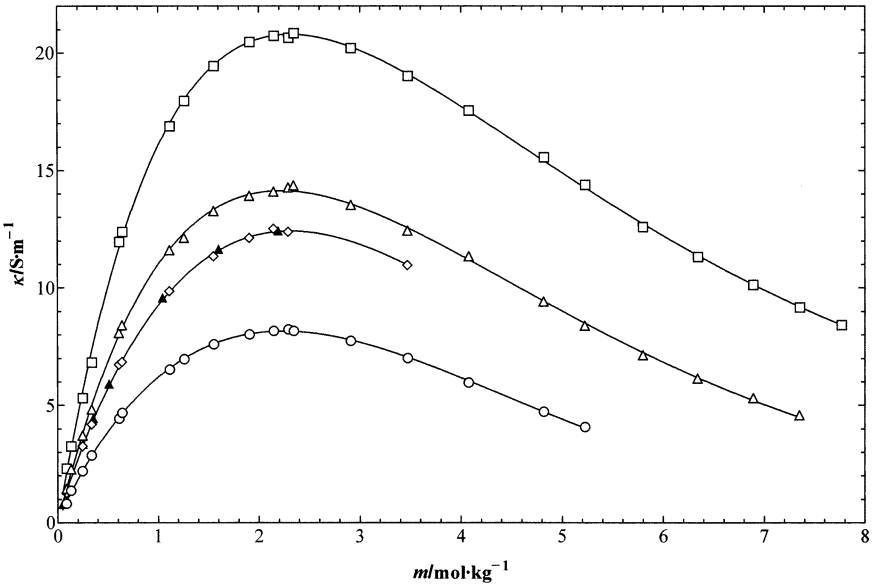


**Figure 2.** Plots of electrical conductivity, $\kappa$, versus molality, $m$, at (○) 273.15 K, (◇) 291.15 K, (Δ) 298.15 K, and (□) 323.15 K for aqueous zinc nitrate solutions (symbols and solid curves represent experimental and fitted (from eq 5) values, respectively). (▲) Reference 9.

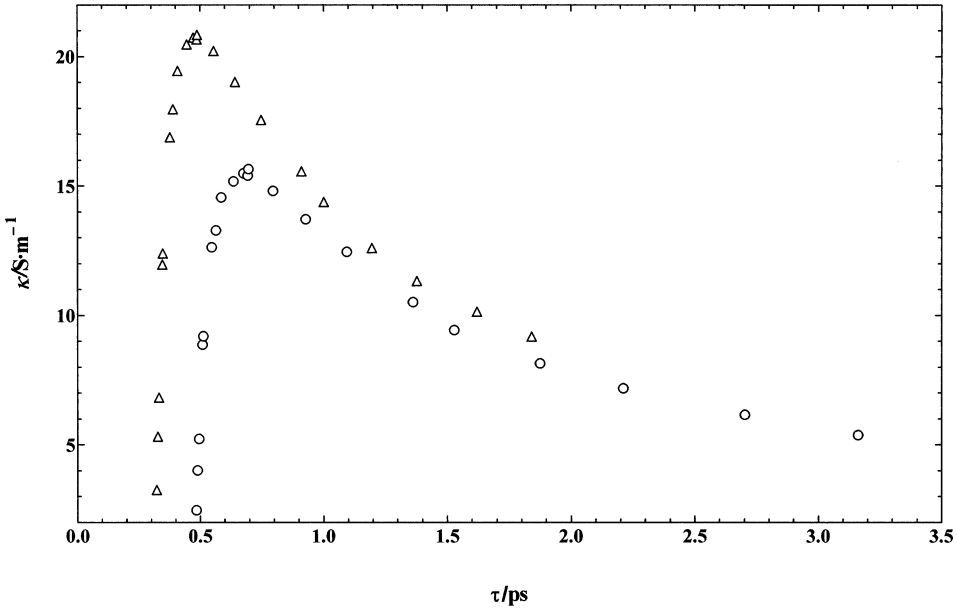


**Figure 3.** Dependence of electrical conductivity, $\kappa$, on shear relaxation time, $\tau$, at (○) 303.15 K and (△) 323.15 K for aqueous zinc nitrate solutions.

surface enthalpy, $H_\sigma$, per unit area are expressed by the following equations:

$$S_\sigma = -\mathrm{d}\sigma/\mathrm{d}T \tag{8}$$

and

$$H_\sigma = \sigma - T(\mathrm{d}\sigma/\mathrm{d}T) \tag{9}$$

where $T$ is the absolute temperature. The parameters $b_3$ and $a_3$ in eq 7 represent $S_\sigma$ and $H_\sigma$, respectively. Figure 4 depicts the plots of both $S_\sigma$ and $H_\sigma$ against concentration. Variation of $H_\sigma$ and $S_\sigma$ with concentration also envisaged some kind of structural changes in aqueous zinc nitrate solutions. Up to ≈2.2 mol·kg$^{-1}$ (Figure 4), $S_\sigma$ decreases but $H_\sigma$ remains almost constant where hydrated ions exist in the solution and the inflection points in both the $S_\sigma$ and $H_\sigma$ versus $m$ plots at ≈2.2 mol·kg$^{-1}$ imply the existence of the most stable species. Beyond ≈2.2 mol·kg$^{-1}$, both $H_\sigma$ and $S_\sigma$ rise sharply with concentration, indicating configurational changes and accounting for the predominant existence of solvent-separated and/or solvent-shared ion pairs. Bloom et al.[33] proposed a correlation of bonding character

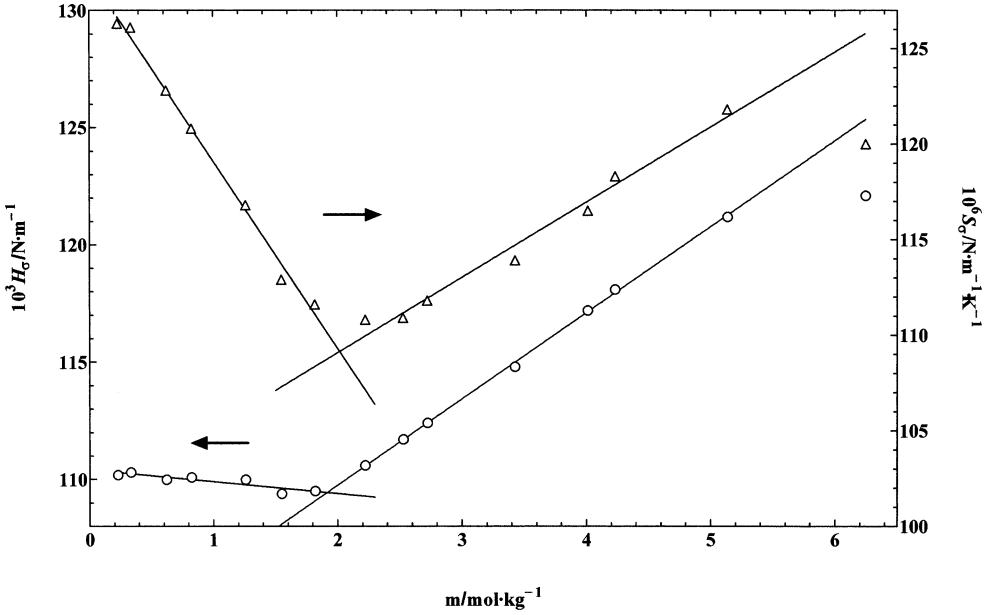


**Figure 4.** Variation of surface enthalpy, (○) $H_\sigma$, and surface entropy, (△) $S_\sigma$, per unit area with molality, $m$, for aqueous zinc nitrate solutions. The solid lines are guides to the eyes.

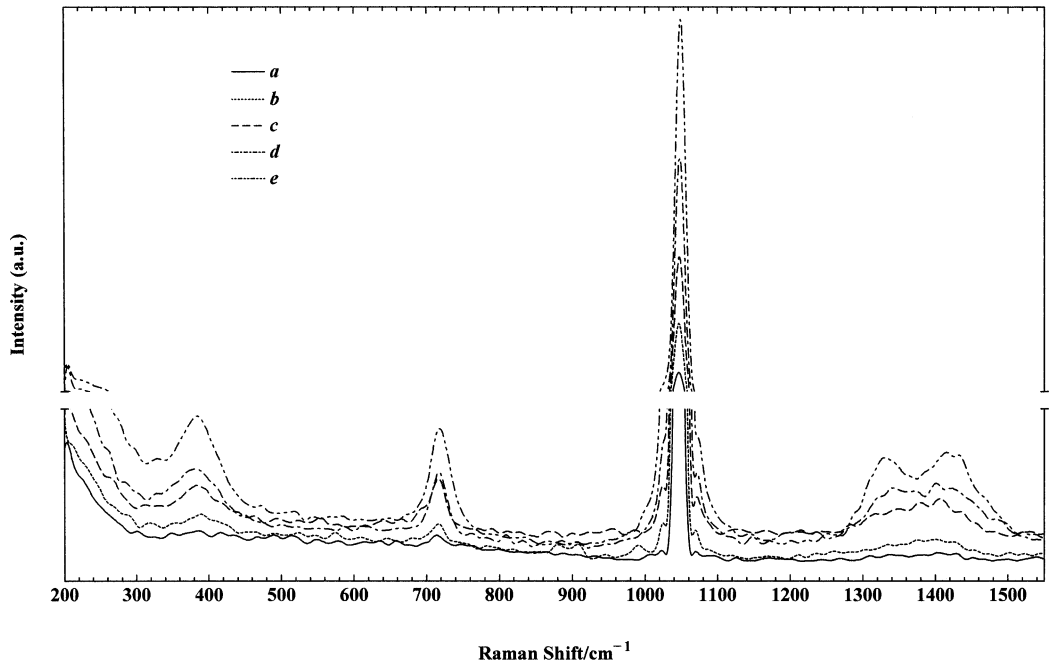


**Figure 5.** Raman spectra of (a) 0.3340, (b) 0.8228, (c) 2.188, (d) 3.426, and (e) 5.973 mol·kg$^{-1}$ aqueous zinc nitrate solutions in the frequency range from 200 to 1600 cm$^{-1}$ at room temperature.

(ionic or covalent) from the magnitude of $H_\sigma$. However, the magnitude of $H_\sigma$ for pure water[34] and that of the concentrated zinc nitrate solutions (Table 4) are comparable. Such a correlation could not be established from the data, as was pointed out by other authors.[34,35]

***Raman Spectra.*** The Raman spectra of aqueous zinc nitrate solutions in the concentration range from (0.3340 to 5.973) mol·kg$^{-1}$ are depicted in Figure 5. The band parameters for the nitrate modes and the libration band of water are listed in Table 5. The band at ≈390 cm$^{-1}$ is very weak for 0.3340 mol·kg$^{-1}$ but becomes sharp with increased intensity as the concentration is increased. This band was reported for aqueous solutions as well as hydrated zinc nitrate melt and $Zn(NO_3)_2 \cdot 6H_2O$ crystal where zinc is octahedrally coordinated by water.[5,36] The band is assigned to a $Zn^{2+}-OH_2$ stretching mode ($\nu_{lib}$) (libration band), the presence of which represents the strong cation−water interactions.

The nitrate deformation band ($\nu_4$) at ≈713 cm$^{-1}$ for free $NO_3^-$ ion is shifted to a higher frequency region by ≈3 cm$^{-1}$ with increased intensity as the concentration is increased. The intensity of the band is increased sharply for 2.188 mol·kg$^{-1}$ and above. The frequency shift is accounted for the $H_2O-NO_3^-$ interaction. The splitting of the $\nu_4$ band for aqueous $Zn(NO_3)_2$ solution begins to occur at ≈9.3 mol·kg$^{-1}$ ($Zn(NO_3)_2 \cdot 6H_2O$) and beyond and appears at (720 and 750) cm$^{-1}$.[5] We have recorded Raman spectra up to ≈6 mol·kg$^{-1}$ in the present study, and a single symmetrical band at (716 ± 3) cm$^{-1}$ has been observed (Figure 5).

The intensity and full-width at half-height (fwhh) of the symmetric stretching mode ($\nu_1$) of nitrate at 1048 cm$^{-1}$ increase with concentration, but the position of the peak

**Table 4. Least-Squares Fitted Values of the Constant Parameters of Eq 7 for Aqueous Zinc Nitrate Solutions**

| $m$/mol·kg$^{-1}$ | $10^3a_3$/N·m$^{-1}$ | $10^6b_3$/N·m$^{-1}$·K$^{-1}$ | std dev in $\sigma$ |
|---|---|---|---|
| 0.2263 | 110.2 ± 0.3 | 126.3 ± 1.0 | 0.03 |
| 0.3340 | 110.3 ± 0.7 | 126.1 ± 2.5 | 0.07 |
| 0.6198 | 110.0 ± 0.7 | 122.8 ± 2.3 | 0.06 |
| 0.8228 | 110.1 ± 1.0 | 120.8 ± 3.3 | 0.09 |
| 1.259 | 110.0 ± 1.0 | 116.8 ± 3.6 | 0.10 |
| 1.549 | 109.4 ± 0.4 | 112.9 ± 1.2 | 0.03 |
| 1.818 | 109.5 ± 0.8 | 111.6 ± 2.7 | 0.07 |
| 2.222 | 110.6 ± 0.9 | 110.8 ± 3.0 | 0.08 |
| 2.526 | 111.7 ± 1.7 | 110.9 ± 5.7 | 0.16 |
| 2.721 | 112.4 ± 1.2 | 111.8 ± 4.0 | 0.11 |
| 3.426 | 114.8 ± 0.6 | 113.9 ± 2.2 | 0.06 |
| 4.011 | 117.2 ± 1.1 | 116.5 ± 3.7 | 0.10 |
| 4.231 | 118.1 ± 0.3 | 118.3 ± 1.1 | 0.03 |
| 5.133 | 121.2 ± 1.3 | 121.8 ± 4.6 | 0.13 |
| 6.245 | 122.1 ± 2.1 | 120.0 ± 7.1 | 0.11 |

**Table 5. Band Parameters Corresponding to Nitrate Modes and the Libration Band ($\nu_{lib}$) of Water for Aqueous Zinc Nitrate Solutions at Room Temperature**

| | peak position[a] (cm$^{-1}$) | | | | |
|---|---|---|---|---|---|
| mode | $m$ = 0.3340 mol·kg$^{-1}$ | $m$ = 0.8228 mol·kg$^{-1}$ | $m$ = 2.188 mol·kg$^{-1}$ | $m$ = 3.426 mol·kg$^{-1}$ | $m$ = 5.973 mol·kg$^{-1}$ |
| $\nu_{lib}$ | 386 (vw) | 389 (w) | 383 (s) | 382 (s) | 384 (vs) |
| $\nu_1$ | 1047 (vs) | 1047 (vs) | 1048 (vs) | 1048 (vs) | 1049 (vs) |
| $\nu_3$ | 1404 (vw) | 1401 (vw) | 1406 (b) | 1341 (m) | 1329 (s) |
| | | | | 1401 (m) | 1415 (s) |
| $\nu_4$ | 714 (w) | 716 (w) | 716 (s) | 717 (s) | 718 (vs) |

[a] b, broad; m, medium; w, weak; vw, very weak; s, sharp; vs, very sharp.

frequency for all solutions does not change. A similar observation has been reported by Sze and Irish.[5]

The intensity of the envelope at ≈1400 cm$^{-1}$ corresponding to the asymmetric stretching mode ($\nu_3$) of nitrate increases as the concentration is increased. Though the envelope begins to appear at 0.8228 mol·kg$^{-1}$ solution, the band splitting occurs at 2.188 mol·kg$^{-1}$ and becomes distinguished for 3.426 mol·kg$^{-1}$ zinc nitrate solution. At 3.426 mol·kg$^{-1}$, the two bands appear at (1341 and 1401) cm$^{-1}$ with separation, $\Delta\nu$ = 60 cm$^{-1}$. For 5.973 mol·kg$^{-1}$ zinc nitrate solution the band separation further enhanced (separation $\Delta\nu$ = 86 cm$^{-1}$) and was centered at (1329 and 1415) cm$^{-1}$. The splitting pattern of the $\nu_3$ band was also observed for other nitrate salts.[37−39] Irish and Walrafen[39] in their studies concluded that water causes the splitting ($\nu_3$ band) and proposed an interaction of the type, for example, $Ca^{2+}-(H_2O)_x-NO_3^-$ (solvent-separated ion pairs).

The bands at (384, 718, 1049, 1329, and 1415) cm$^{-1}$ suggest that $NO_3^-$ ion is not entering in the first coordination sphere of $Zn^{2+}$ ion.[5] From the variation of $\Delta\nu$ versus $C^{1/3}$ ($\Delta\nu$ of 1400 cm$^{-1}$ region), Sze and Irish[5] suggested that the outer-sphere ion pair formation increases rapidly at around 6.2 mol·kg$^{-1}$. From the variation of $\kappa$ versus $\tau$ plots (Figure 3), it is apparent that the changing of the slope occurs in the higher concentration region at ≈5.8 mol·kg$^{-1}$ ($\tau$ = 1.874 ps at 303.15 K and $\tau$ = 1.194 ps at 323.15 K). Therefore, it is suggested that the hydrated $Zn^{2+}$ and $NO_3^-$ ions in the concentration range from dilute to 2.2 mol·kg$^{-1}$ and beyond 2.2 mol·kg$^{-1}$ solvent-shared and/or solvent-separated ion pairs govern the transport process.

## Acknowledgment

The authors express their gratitude to the Director of the laboratory for the facilities and interest in this work. The authors are also indebted to the Indian Association for the Cultivation of Science, Kolkata, for recording the Raman spectra.

## Supporting Information Available:

Tables of measured densities, speeds of sound in aqueous zinc nitrate solutions as functions of concentration and temperature, electrical conductivities of aqueous zinc nitrate solutions as functions of concentration and temperature, measured viscosities of aqueous zinc nitrate solutions at various concentrations and temperatures, and surface tensions of aqueous zinc nitrate solutions measured at different temperatures as a function of concentration. This material is available free of charge via the Internet at http://pubs.acs.org.

## Literature Cited

(1) Wahab, A.; Mahiuddin, S. Isentropic Compressibility and Viscosity of Aqueous and Methanolic Calcium Chloride Solutions. *J. Chem. Eng. Data* **2001**, *46*, 1457−1463.
(2) Rohman, N.; Dass, N. N.; Mahiuddin, S. Isentropic Compressibility of Aqueous and Methanolic Sodium Thiocyanate Solutions. *J. Chem. Eng. Data* **1999**, *44*, 465−472.
(3) Rohman, N.; Wahab, A.; Dass, N. N.; Mahiuddin, S. Viscosity, Electrical Conductivity, Shear Relaxation Time and Raman Spectra of Aqueous and Methanolic Sodium Thiocyanate Solutions. *Fluid Phase Equilib.* **2001**, *178*, 277−297.
(4) Wahab, A.; Mahiuddin, S. Isentropic Compressibility and Viscosity of Aqueous and Methanolic Lithium Chloride Solutions. *Can. J. Chem.* **2002**, *80*, 175−182.
(5) Sze, Y.-K.; Irish, D. E. Vibration Spectral Studies of Ion-Ion and Ion−solvent Interactions. I. Zinc Nitrate in Water. *J. Solution Chem.* **1978**, *7*, 395−415.
(6) Jain, S. K.; Jain, A. K.; Gupta, A. K.; Singh, V. V. Densities and Refractive Indices of Aqueous Zinc Nitrate Solutions. *J. Chem. Eng. Data* **1985**, *30*, 301−304.
(7) Doan, T. H.; Sangster, J. Viscosities of Concentrated Aqueous Solutions of Some 1:1, 2:1 and 3:1 Nitrates at 25 °C. *J. Chem. Eng. Data* **1981**, *26*, 141−144.
(8) Carpio, R.; Mehicic, M.; Borsay, F.; Petrovic, C.; Yeager, E. Investigation of Aqueous Calcium Nitrate, Zinc Nitrate, and Zinc Chloride Solutions Using Acoustic Velocity Measurements. *J. Phys. Chem.* **1982**, *86*, 4980−4987.
(9) Washburn, E. W., Ed. *International Critical Tables of Numerical Data, Physics, Chemistry, and Technology*; McGraw-Hill: New York, 1928; Vol. VI, p 237.
(10) Washburn, E. W., Ed. *International Critical Tables of Numerical Data, Physics, Chemistry, and Technology*; McGraw-Hill: New York, 1928; Vol. IV, p 464.
(11) Kumar, A. Speed of Sound in Concentrated Aqueous KCl Solutions from 278.15 to 338.15 K. *J. Chem. Eng. Data* **2003**, *48*, 388−391.
(12) Bowen, D. E.; Priesand, M. A.; Feighny, S. R. Ultrasound Propagation in $NH_3-H_2O$ Mixtures. *J. Chem. Phys.* **1975**, *62*, 808−814.
(13) Ohtaki, H.; Radnai, T. Structure and Dynamics of Hydrated Ions. *Chem. Rev.* **1993**, *93*, 1157−1204.
(14) Ohtaki, H.; Yamaguchi, T.; Maeda, M. X-ray Diffraction Studies of the Structures of Hydrated Divalent Transition-Metal Ions in Aqueous Solution. *Bull. Chem. Soc. Jpn.* **1976**, *49*, 701−708.
(15) Bol, W.; Gerrits, G. J. A.; van Panthaleon van Eck, C. L. The Hydration of Divalent Cations in Aqueous Solution. An X-ray Investigation with Isomorphous Replacement. *J. Appl. Crystallogr.* **1970**, *3*, 486-492.
(16) Dagnall, S. P.; Hague, D. N.; Towl, A. D. C. X-ray Diffraction Study of Aqueous Zinc(II) Nitrate. *J. Chem. Soc., Faraday Trans. 2* **1982**, *78*, 2161−2167.
(17) Powell, D. H.; Gullidge, P. M. N.; Neilson, G. W.; Bellissent-Funel, M. C. Zinc(2+) Hydration and Complexation in Aqueous Electrolyte Solutions. *Mol. Phys.* **1990**, *71*, 1107−1116.
(18) Sakane, H.; Miyanaga, T.; Watanabe, I.; Matsubayashi, N.; Ikeda, S.; Yokoyama, Y. Reproducibility Tests of Extended X-ray absorption Fine structure for Aqua and Ammine Complexes of First Transition Metals in Solid and Aqueous Solution. *Jpn. J. Appl. Phys.* **1993**, *32*, 4641−4647.
(19) Muñoz-Páez, A.; Pappalardo, R. R.; Sachez Marcos, E. Determination of Second Hydration Shell of $Cr^{3+}$ and $Zn^{2+}$ in Aqueous Solutions by Extended X-ray Absorption Fine Structure. *J. Am. Chem. Soc.* **1995**, *117*, 11710−11720.
(20) Bulmer, J. T.; Irish, D. E.; Ödberg, L. The Temperature Dependence of Raman Band Parameters for Aquated Mg(II) and Zn(II). *Can. J. Chem.* **1975**, *53*, 3806−3811.
(21) Ikushima, Y.; Saito, N.; Arai, M. Raman Spectral Studies of Aqueous Zinc Nitrate Solution at High Temperatures and at a High Pressure of 30 MPa. *J. Phys. Chem. B* **1998**, *102*, 3029−3035.
(22) Chillemi, G.; D'Angelo, P.; Pavel, N. V.; Sanna, N.; Barone, V. Development and Validation of an Integrated Computational Approach for the Study of Ionic Species in Solution by Means of Effective Two-Body Potentials. The Case of $Zn^{2+}$, $Ni^{2+}$, and $Co^{2+}$ in Aqueous Solutions. *J. Am. Chem. Soc.* **2002**, *124*, 1968−1976.

(23) Yongyai, Y. P.; Kokpol, S.; Rode, B. M. Zinc Ion in Water: Intermolecular Potential with Approximate Three-Body Correction and Monte Carlo Simulation. *Chem. Phys.* **1991**, *156*, 403−412.
(24) Marini, G. W.; Texler, N. R.; Rode, B. M. Monte Carlo Simulations of Zn(II) in Water Including Three-Body Effects. *J. Phys. Chem.* **1996**, *100*, 6808−6813.
(25) Bock, C. W.; Katz, A. K.; Glusker, J. P. Hydration of Zinc Ions: A Comparison with Magnesium and Beryllium Ions. *J. Am. Chem. Soc.* **1995**, *117*, 3754−3765.
(26) Rudolph, W. W.; Pye, C. C. Zinc(II) Hydration in Aqueous Solution. A Raman Spectroscopic Investigation and an Ab Initio Molecular Orbital Study. *Phys. Chem. Chem. Phys.* **1999**, *1*, 4583−4593.
(27) Lee, S.; Kim, J.; Park, J. K.; Kim, K. S. Ab Initio Study of the Structures, Energetics, and Spectra of Aquazinc(II). *J. Phys. Chem.* **1996**, *100*, 14329−14338.
(28) Pavlov, M. P.; Siegbahn, E. M.; Sandström, M. Hydration of Beryllium, Magnesium, Calcium, and Zinc Ions Using Density Functional Theory. *J. Phys. Chem. A* **1998**, *102*, 219−228.
(29) Bock, C. W.; Katz, A. K.; Markham, G. D.; Glusker, J. P. Manganese as a Replacement for Magnesium and Zinc: Functional Comparison of the Divalent Ions. *J. Am. Chem. Soc.* **1999**, *121*, 7360−7372.
(30) Hartmann, M.; Clark, T.; van Eldik, R. Hydration and Water Exchange of Zinc(II) Ions. Application of Density Functional Theory. *J. Am. Chem. Soc.* **1997**, *119*, 7843−7850.
(31) Dudev, T.; Lim, C. Tetrahedral vs Octahedral Zinc Complexes with Ligands of Biological Interest: A DFT/CDM Study. *J. Am. Chem. Soc.* **2000**, *122*, 11146−11153.
(32) Casteel, J. F.; Amis, E. S. Specific Conductance of Concentrated Solutions of Magnesium Salts in Water-Ethanol System. *J. Chem. Eng. Data* **1972**, *17*, 55−59.
(33) Bloom, H.; Davis, F. G.; James, D. W. Molten Salt Mixtures. IV. Surface Tension and Surface Heat Content of Molten Salts and Their Mixtures. *Trans. Faraday Soc.* **1960**, *56*, 1179−1186.
(34) Abraham, M.; Abraham, M.-C.; Ziogas, I. Surface Tension of Liquids from Molten Nitrate Mixtures to Water. *J. Am. Chem. Soc.* **1991**, *113*, 8583−8590.
(35) Kumar, A. Surface Tension, Viscosity, Vapor Pressure, Density, and Sound Velocity for a Miscible Continuously from a Pure Fused Electrolyte to a Nonaqueous Liquid with a Low Dielectric Constant: Anisole with Tetra-*n*-Butylammonium Picrate. *J. Am. Chem. Soc.* **1993**, *115*, 9243−9248.
(36) Brooker, M. H.; Irish, D. E. Vibrational Spectral Studies of Hexaquozinc Nitrate and Deuterated Hexaquozinc Nitrate-$d_2$. *Can. J. Chem.* **1971**, *49*, 1510−1514.
(37) Irish, D. E.; Davis, A. R.; Plane, R. A. Types of Interaction in Some Aqueous Metal Nitrate Systems. *J. Chem. Phys.* **1969**, *50*, 2262−2263.
(38) Hester, R. E.; Plane, R. A. Raman Spectrophotometric Study of Complex Formation in Aqueous Solutions of Calcium Nitrate. *J. Chem. Phys.* **1964**, *40*, 411−414.
(39) Irish, D. E.; Walrafen, G. E. Raman and Infrared Spectral Studies of Aqueous Calcium Nitrate Solutions. *J. Chem. Phys.* **1967**, *46*, 378−384.

Received for review July 2, 2003. Accepted September 25, 2003. A.W. is grateful to the Council of Scientific and Industrial Research, New Delhi, for the award of a senior research fellowship.

JE0302001